RSC Advances

PAPER

View Article Online
View Journal | View Issue

Cite this: *RSC Adv.*, 2024, **14**, 23710

A novel strategy combining hydrogenotrophic methanogens' bioaugmentation and biochar biostimulation for simultaneous polycyclic aromatic hydrocarbon biodegradation and bioenergy recovery

Rui Tang, Min Zhang and Xin Li *

A novel strategy combining bioaugmentation using methanogenic archaea and biostimulation using biochar was proposed for the first time to obtain simultaneous improvement of mixed PAHs' anaerobic biodegradation and bioenergy production. The results showed that the addition of PHAs immediately resulted in inhibition in methane production and accumulation of VFA, indicating that PHAs are more toxic to methanogens than the acetogenic bacteria. The coupling of biochar with hydrogenotrophic methanogen alleviated the inhibitory effects of PAHs, allowing the anaerobic fermentation system to recover its methane production capability rapidly. Compared to the Fe^{3+} + bioaugmentation group, the biochar + bioaugmentation group exhibited a 7.5% higher restored cumulative methane production. This coupling strategy ultimately facilitated the degradation of most PAHs, achieving a removal rate of over 90%. Moreover, the coupled biochar and bioaugmentation induced significant changes in the archaeal community structure. Direct interspecies electron guilds (*i.e.*, *Streptococcus* and *Methanosarcina*) were enriched in the presence of biochar and bioaugmentation, responsible for prominent PAH removal and methane recovery. This study demonstrated the feasibility of simultaneous PAH biodegradation and bioenergy production using electron acceptor and enriched microorganisms.

Received 21st May 2024
Accepted 23rd July 2024

DOI: 10.1039/d4ra03732d

rsc.li/rsc-advances

1. Introduction

Polycyclic aromatic hydrocarbons (PAHs) are carcinogenic and mutagenic compounds, that are generated by human actions such as emissions from burning fossil fuels or wastewater from industrial operations, agricultural practices, and domestic heating. After migrating into wastewater, PAHs may accumulate in sediments due to their limited solubility in water and hydrophobic characteristics, leading to subsequent soil contamination. According to research findings, PAHs have a toxic effect on microorganisms in the subsequent sewage treatment process, and trace amounts of PAHs can lead to microbial inactivation.[1] Therefore, correctly and efficiently treating wastewater containing PAHs is necessary and urgent before being discharged into the environment.

Many physical and chemical methods, such as volatilization,[2] photodegradation,[3] chemical oxidation,[4] and solubilization-elution technology,[5] have been employed for PAH removal. Their application is constrained by the elevated costs, residual pollutants, and the potential secondary pollution. In comparison, microbial degradation of PAHs is gaining attention due to its eco-friendly, sustainable, and cost-effective advantages.

PAHs can be categorized based on benzene ring numbers, with 2–3 rings classified as low molecular weight (LMW-PAHs) and 4–7 rings as high molecular weight (HMW-PAHs). Previous research has primarily focused on the decomposition of LMW-PAHs or a specific HMW-PAH.[6] In wastewater, such as petroleum hydrocarbons and pyrolysis oil, PAHs are often a mixture of multiple compounds. The HMW-PAHs exhibit greater resistance and toxicity to living organisms compared to the LMW-PAHs.[3] Nevertheless, there is limited documentation on the anaerobic biodegradation of mixed PAHs and scarce literature on the anaerobic degradation of mixed HMW-PAHs.

For PAH biodegradation (biomineralization), a terminal electron acceptor (TEA) is needed. PAHs biomineralization is efficient in aerobic conditions using O_2 as TEA. In anaerobic conditions, alternate TEAs such as nitrate,[7] sulfate,[8] and Fe(III)[9] can enhance PAHs degradation efficiently. However, additional TEA should be added to the anaerobic system to treat extensive or high concentrations of PAHs wastewater. This may cause secondary pollution. Alternatively, biochar has been recognized as a conductive material mediating direct interspecies electron

College of Engineering, China Agricultural University (Key Laboratory for Clean Renewable Energy Utilization Technology, Ministry of Agriculture), No. 17 Qinghua Donglu, Haidian District, Beijing 100083, People's Republic of China. E-mail: lxin@cau.edu.cn; Fax: +86 (10) 62737858; Tel: +86 (10) 62737858

transfer (DIET).[10] Biochar is an eco-friendly and low-cost conductive material. Microbial degradation of PAHs may be facilitated by biochar.[11]

Another crucial factor influencing PAHs biodegradation efficiency is the prevalence of functional microorganisms. Implementing a bioaugmentation dosage is a viable approach for efficient biodegradation of PAHs. Previous studies have researched improving PAHs biodegradation by adding specific microbial strains extracted from soils contaminated with PAHs or crude oil.[12,13] However, the biodegradation efficiency of these strains was found to be unstable.[5] The research community has also focused on using bacteria strains, such as *Rhodocccus erythropolis* and *Pseudomonas stuzeri*,[2] or a defined bacteria consortium for bioaugmentation. However, pure functional microorganisms are difficult to apply to real PAH-contaminated sites. Researchers have reported that a mixed bacterial consortium shows enhanced degradation of mixed PAHs compared to a single strain, due to its versatile enzymatic and metabolic functions.[14] Additionally, Bianco *et al.* (2020) found that the methanogenic phase has a greater impact on PAH degradation than the acidogenic phase.[15] However, there is a lack of literature on studies investigating the evidence of evolution of the archaeal community during PAH anaerobic digestion. Furthermore, no studies have focused on the correlation between PAH degradation and methanogenic archaea bioaugmentation.

Therefore, this study proposed a novel strategy that combines bioaugmentation using methanogenic archaea and biostimulation using biochar for the first time, aiming to achieve simultaneous improvement in mixed PAHs anaerobic biodegradation and bioenergy production. Additionally, the study elucidated the microbial community changes during the anaerobic digestion of PAHs. This study aimed to provide an interdisciplinary overview of the anaerobic biodegradation of mixed PAHs.

Table 1 PAHs used in this study

Compounds	Structure	M (g mol^{-1})
Naphthalene		128.18
Acenaphthylene		152.20
Acenaphthene		154.20
Fluorene		166.23
Phenanthrene		178.24
Anthracene		178.24
Fluoranthene		202.26
Pyrene		202.26
Benzo[*a*]anthracene		228.30
Chrysene		228.30
Benzo[*b*]fluoranthene		252.32
Benzo[*k*]fluoranthene		252.32
Benzo[*a*]pyrene		252.32
Indeno[1,2,3-*cd*]pyrene		276.34
Dibenzo[*a*,*h*]anthracene		278.35
Benzo[*g*.*h*.*i*]perylene		276.34

2. Materials and methods

2.1 Preparation of PAH solution

In total, 16 PAHs (6 LMW-PAHs and 10 HMW-PAHs) were used in this study. All PAHs were dissolved in *n*-hexane to make the PAH-contained solution with a final concentration of 10 mg L^{-1} for each PAH (Table 1). The total concentration of 16 types of PAHs is 160 mg L^{-1}. On day 10, 100 mL of the solution was added to the reactors.

2.2 Preparation of biochar and enrichment of bioaugmentation dosages

Cattle manure (CM) was used in the production of biochar. The CM was collected from a dairy farm in Beijing, China. Following washing, CM was dried in an oven at 105 °C for 24 h. Biochar was derived from CM through slow pyrolysis in a tubular furnace, with a final temperature set at 600 °C. The pyrolysis process had a heating rate of 10 °C min^{-1}. After reaching the final pyrolysis temperature, the final temperature was maintained for 1 h. During pyrolysis, a constant N_2 stream (0.2 L min^{-1}) was purged to guarantee an oxygen-limited environment. When pyrolysis ended, biochar was cooled below 100 °C and transferred into desiccators before use.

According to Wang *et al.* (2023), the enrichment process of hydrogenotrophic methanogens (HM) serving as bioaugmentation dosage was carried out.[16] The enrichment process progressed in a continuous stirred tank reactor (CSTR) using CM as the substrate. In the meantime, external H_2 was introduced through an air stone diffuser and circulated along with the generated biogas throughout a 24 hours batch cycle. After 80 days, methane content reached up to 95%, and the HM consortium was obtained. Before the start of the test, the microbial flora was cultivated in a liquid medium, and the concentration of the microorganisms in the medium was determined to be approximately 5×10^3 to 8×10^3 CFU mL^{-1}.

2.3 Anaerobic biodegradation test of PAHs

Anaerobic digestion of PAHs was carried out in 1 L laboratory-scale CSTRs. The temperature was maintained at 37 ± 2 °C with a water bath. Inoculum was collected from a biogas facility supplied with municipal wastewater in Beijing. Before utilization, the inoculum was stored under anaerobic conditions until there was no traceable gas. The specific traits of the inoculum are outlined in Table 2.

Table 2 The characteristics of the inoculum[a]

Parameters	Unit	Inoculum Average ± SD
TS	g L^{-1}	59.08 ± 0.18
VS	g L^{-1}	43.26 ± 0.11
SS	g L^{-1}	49.45 ± 0.53
VSS	g L^{-1}	19.74 ± 0.12
pH	—	7.84 ± 0.19
TCOD	mg L^{-1}	47.24 ± 3.05
SCOD	mg L^{-1}	23.37 ± 0.66
NH_4^+–N	mg L^{-1}	857 ± 21

[a] '—': not available. TS: total solid; VS: volatile solid; SS: suspended solid; VSS: volatile suspended solid; TCOD: total chemical oxygen demand.

Five treatment reactors were established in this experiment. The first treatment reactor was fed with 5 g glucose every day and served as the control reactor (R_{CK}). The second treatment reactor was fed with 5 g glucose every day, and PAHs were added on day 10. Later, $FeCl_3$ was added on day 15 to reach a final concentration of 0.1 mg L^{-1} and 10 mL HM was added on day 26 (R_{Fe+HM}). The third treatment reactor was fed with 5 g glucose every day, and PAHs were added on day 10. Later, BC was added on day 15 to reach a final concentration of 0.5 g L^{-1}, and HM was added on day 26 (R_{BC+HM}). The fourth treatment reactor was fed with 5 g glucose every day; PAHs were added on day 10. Then, the reactors received BC only on day 15 (R_{BC}). The fifth treatment reactor was fed with 5 g glucose every day; PAHs were added on day 10; and then, reactors received HM only on day 26 (R_{HM}). All the reactors were operated for 43 days.

The reactors were operated in a fed-batch mode. The effluent from the reactor was used to dissolve glucose for feeding, with only a minimal quantity of liquid in the reactor being allocated for testing purposes. This was done to prevent the loss of PAHs during feeding and discharge.

2.4 Analytical methods

Gas composition (CH_4 and CO_2) was analyzed by gas chromatograph (Shimadzum GC-8A, Japan). Liquid samples used for VFA measurement were collected through filtration through a 0.45 μm filter after centrifuging at 8000 rpm for 20 minutes (TGL-16 M, China). VFAs were analyzed by Gas Chromatograph (Shimadzu, GC-2010 Plus, Japan).[16]

After sample collection, 20 g of fresh samples were taken and dehydrated using a vacuum freeze dryer, then ground into fine particles of about 1 mm. PAHs and metabolites were determined as described by Mu *et al.* (2022). The freeze-dried samples were transferred to a 150 mL conical flask. 50 mL solution of dichloromethane and *n*-hexane (1 : 1) was added to the flask and ultrasonic extraction was carried out with the precipitate for 30 min. Then, the flask was allowed to stand for 10 min to separate into two layers. The supernatant was collected, and the residual samples were supplemented with 50 mL of extract solution and subjected to ultrasonic extraction again. The operation was repeated twice. Eventually, three extracts were combined, purified, and dehydrated with anhydrous sodium sulfate.[17]

Concentrations of PAHs were determined through the following procedure: PAHs were identified using a GC/MS system (Agilent GC/MSD 7890B, USA). Helium was the carrier gas with a 1.2 mL min^{-1} flow rate. The injector and transfer line temperatures were held at 280 °C and 300 °C, respectively. The mass spectrometer operated in electron ionization (EI) mode at 70 eV, scanning within the range of 30–600 m/z. Standard curves for each compound were established by injecting a mixture of 16 PAHs (Mix A, Sigma Aldrich, Italy). All samples were measured in triplicates, and the results were exhibited as the mean of the triplicates.

2.5 Microbial analysis

Total DNA was extracted using an E.Z.N.A.® soil DNA kit (Omega Biotek, USA). Primers 338F (5′-ACTCCTACGGGAGGCAGCAG-3′) and 806R (5′-GGACTACHVGGGTWTCTAAT-3′) were used to amplify bacterial 16S rRNA gene V3–V4 variable region. Primers 524F (5′-TGYCAGCCGCCGCGGTAA-3′) and 958R (5′-YCCGGCGTTGAVTCCAATT-3′) were used to amplify archaeal 16S rRNA gene V3–V4 variable region. The obtained products were quantified using the Quantus™ Fluorometer (Promega, USA).

The purified PCR products were then used for library construction with the NEXTFLEX Rapid DNA-Seq Kit, followed by sequencing on the MiSeq PE300 platform. Finally, OTU clustering and species classification analyses were performed on the Majorbio Cloud Platform based on the practical data.

2.6 Predicated gene expression analysis

The Phylogenetic Investigation of Communities by Reconstruction (PICRUSt2) tool was utilized to predict the gene expression of the microbial community. All sequences were annotated against the Kyoto Encyclopedia of Genes and Genomes databases using PICRUSt2 to predict gene functions. The presumed function of microbial communities was determined based on their taxonomic composition.

3. Results and discussion

3.1 Influence of PAHs on anaerobic digestion performance

The biogas and methane production of each experimental reactor is presented in Fig. 1. During the first ten days before adding the PAHs, there was no significant difference in the biogas and methane production among all the reactors, indicating a comparable performance in all the reactors ($P > 0.05$). After PAHs addition (on day 10), inhibition occurred immediately in the R_{BC}, R_{HM}, R_{Fe+HM}, and R_{BC+HM}. Although reactors received biochar or Fe^{3+} on day 15, biogas production still declined. During 19–27 days, no detectable amounts of gas were produced from these reactors. Results implied that an external electron acceptor alone cannot rapidly alleviate the inhibitory effects of PAHs on anaerobic digestion processes.

Fig. 3 depicts the variations in VFA concentrations within the anaerobic digesters. In R_{CK}, VFA concentrations remained

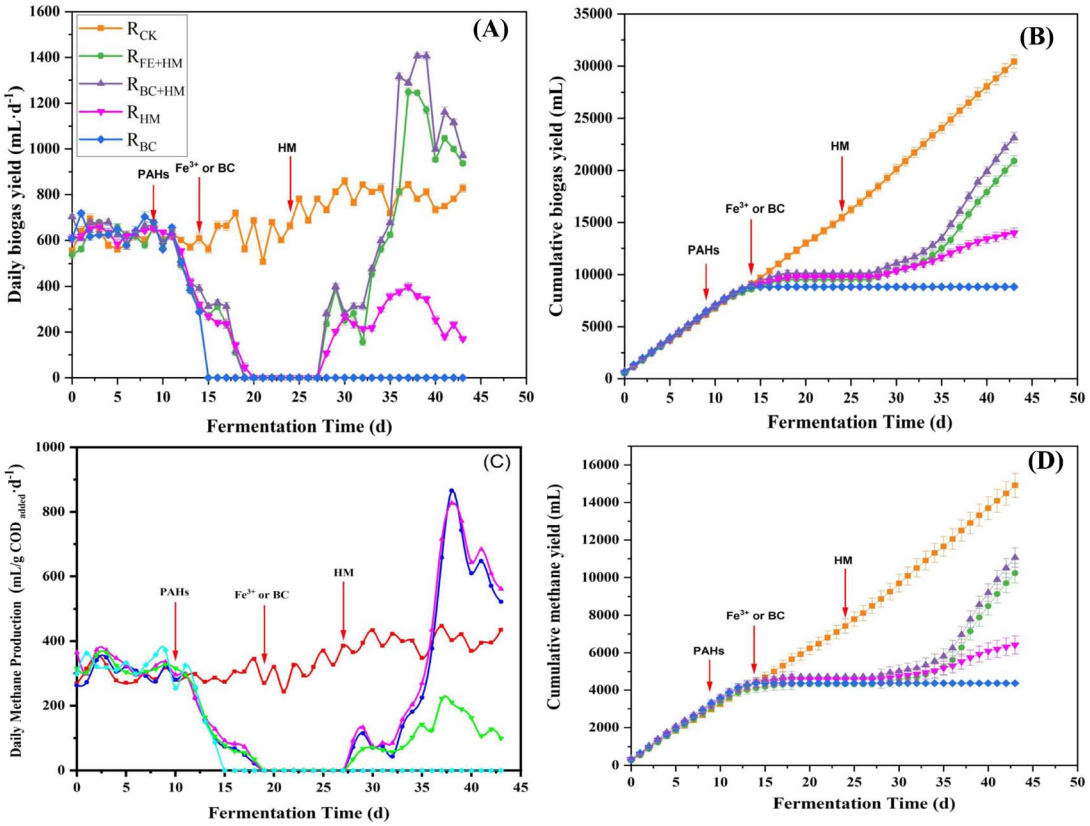

Fig. 1 Daily biogas yield (A), cumulative biogas yield (B), daily methane yield (C), and cumulative methane yield (D) variations during the PAH anaerobic digestion process.

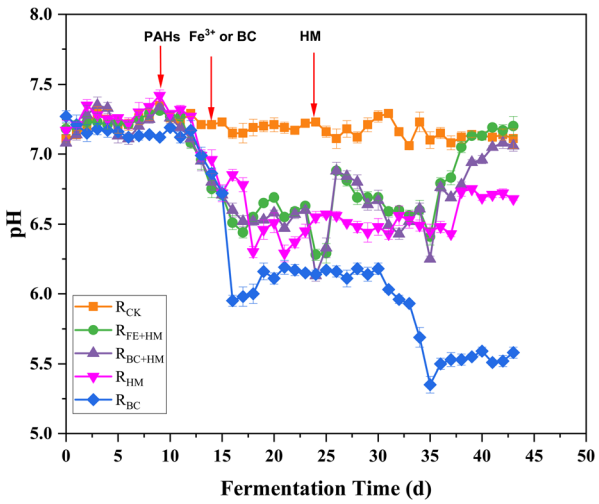

Fig. 2 pH variations during the PAH anaerobic digestion process.

stable at levels below 500 mg L^{-1} throughout the experimental period. In contrast, following the introduction of PAHs on day 10, VFA concentrations exhibited a gradual increase, reaching over 1500 mg L^{-1} on day 15, consistent with a decline in pH in all experimental reactors (Fig. 1 and 2). Concomitantly, VFA concentrations continued to rise significantly, dominated by high concentrations of acetic acid on day 19. The low pH and high total VFA concentration in the reactors receiving PAHs suggested over-acidification and unfavorable conditions as the main reasons for process inhibition.

The stimulatory effect of PAH on VFA production has been affirmed by Chen *et al.* (2022), where a reasonable amount of PAHs could promote acidogenesis, acetogenesis, and methanogenesis in the anaerobic co-digestion of food waste and sludge.[18] Further, Yao *et al.* (2022) claimed that adding naphthalene could promote acidogenesis, but an overdose could induce an imbalance between acidogenesis and methanogenesis, causing a pH imbalance and sabotaging methane production.[19] Methanogenic archaea are more vulnerable to changes in the surrounding environment than bacteria involved in hydrolysis and acidogenesis.[20] Based on the VFA profile analysis, it is suggested that the PAHs may have had a greater toxic effect on the methanogens compared to the acetogenic bacteria (Fig. 3).

3.2 The detoxification effect of combined HM with biochar or Fe^{3+} on PAH biodegradation

On day 25, R_{Fe+HM}, R_{BC+HM}, and R_{HM} were remediated by adding HM. Upon addition, the biogas production in R_{HM}, R_{Fe+HM}, and R_{BC+HM} recovered gradually. Notably, the daily biogas production in R_{Fe+HM} and R_{BC+HM} increased rapidly (Fig. 1). On day 37, the daily biogas production in R_{Fe+HM} and R_{BC+HM} significantly increased, reaching 1249 mL day^{-1} and 1405 mL day^{-1}, respectively. Such phenomenon was due to the degradation of accumulated VFAs consumed by external HM (Fig. 3). The daily

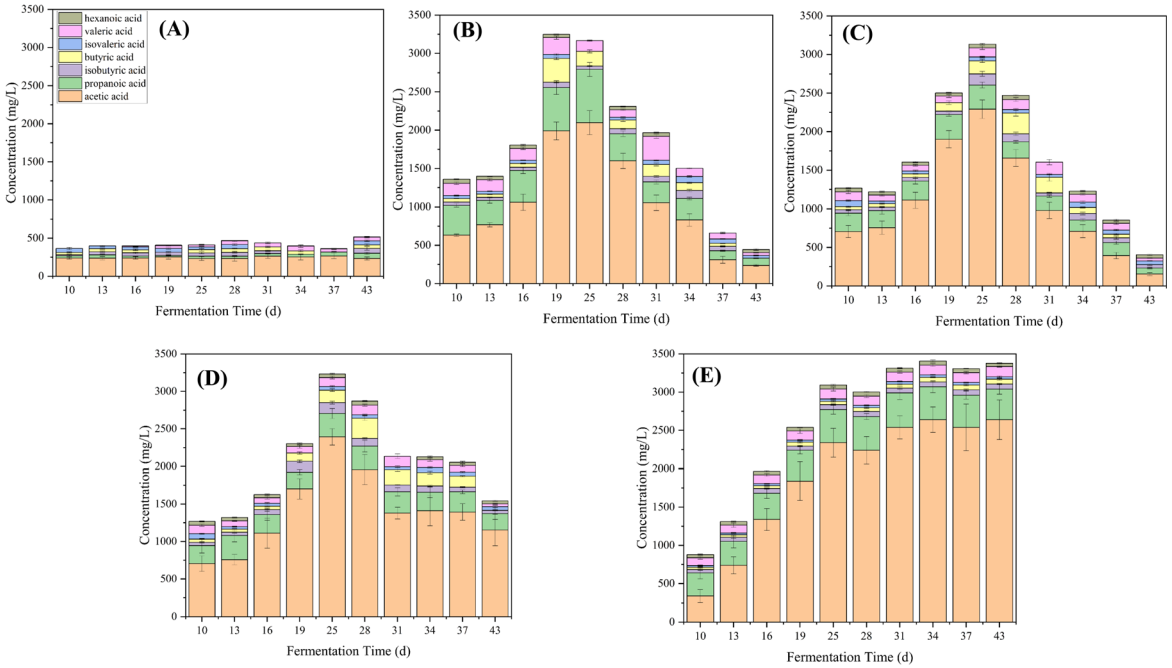

Fig. 3 VFA variations of R_{CK} (A), R_{FE+HM} (B), R_{BC+HM} (C), R_{HM} (D), and R_{BC} (E) during the PAH anaerobic digestion process.

biogas production of R_{HM} also experienced a slight recovery after bioaugmentation with HM, which was significantly lower than that in R_{Fe+HM} and R_{BC+HM}, probably because of the deficiency of TEA in the R_{HM} ($P < 0.05$). While the biogas production in R_{BC} continued to be suppressed, indicating the limited absorption effect of biochar for PAH detoxication (Fig. 1).

The cumulative methane production obtained during 43 days of bioremediation in all reactors is shown in Fig. 1. Because of the toxicity of PAHs, the cumulative biomethane production in reactors with PAHs addition was significantly lower than R_{CK} ($P < 0.05$). Among the PAHs treatment reactors, R_{BC+HM} enjoyed the highest cumulative biomethane production, followed by R_{Fe+HM}, indicating that the detoxication effect of biochar was better than Fe^{3+} in the presence of HM ($P < 0.05$). We hypothesized that the better detoxification effect of biochar may be attributed to the following reasons: first, biochar acts as a shelter for potential bacterial PAH-degraders, which could expediently use PAHs as the carbon source. Second, the conductive properties of biochar enable it to act as an electron acceptor, facilitating the degradation of PAHs.[21]

The strategy can be applied in sewage treatment plants, and treatment for surface water, and groundwater contaminated by PAHs. Another scenario is application for preliminary PAHs removal of industrial wastewater before being discharged into the sewage system. When the biogas production is inhibited by PAHs pollution and acid accumulation occurs, biochar and HM microbial agents could be added to the system every two or three days once time until the biogas production recovers.

3.3 The degradation fate of PAHs during AD

Changes in the concentrations of LMW-PAHs and HMW-PAHs during the anaerobic digestion process are presented in Fig. 4. Results showed that the HMW-PAHs concentration increased to around 7 mg L^{-1} after the addition of PAHs on day 10 and decreased gradually after the addition of Fe^{3+} or biochar on day 15. At the same time, the LMW-PAHs concentrations increased more significantly and reached the peak concentration in each experimental group on day 23 (Fig. 4). The increased concentration of LMW-PAHs might be due to the biotransformation of HMW-PAHs to their sub compounds. After bioaugmenting with HM, the concentrations of HMW-PAHs and LMW-PAHs in R_{Fe+HM} and R_{BC+HM} decreased rapidly, indicating that the PAHs were mineralized to produce methane and CO_2. In the following days, the concentration of PAHs in R_{Fe+HM} and R_{BC+HM} further declined. At the end of the experiment, the removal rates of HMW-PAHs and LMW-PAHs in R_{BC+HM} were the highest, reaching 90.1% and 90.3%, respectively, followed by 82.2% and 74.6% of HMW-PAHs and LMW-PAHs in R_{Fe+HM}, indicating BC coupled with HM had better removal efficiency of PAHs than individuals. Such observation was in accordance with the corresponding biogas and methane production (Fig. 1). In contrast, the removal rates of HMW-PAHs and LMW-PAHs in RHM were 49.6% and 58.7%, respectively. The results indicated that the HM can only promote the biodegradation of PAHs to a certain extent. The lowest removal rate in PAH concentrations was obtained for R_{BC} (HMW-PAHs: 26.7% LMW-PAHs: 18.7%), indicating the limited effect of biochar absorption in removing PAHs. Previous studies have demonstrated the capacity of biochar to adsorb PAHs; however, this adsorption merely facilitates the transfer of PAHs from one medium to another and does not enhance or eliminate the contaminants.[22] Based on the above experimental results, it can be inferred that the degradation of PAHs involved the cleavage of the benzene ring of HMW-PAHs into LMW-PAHs, followed by

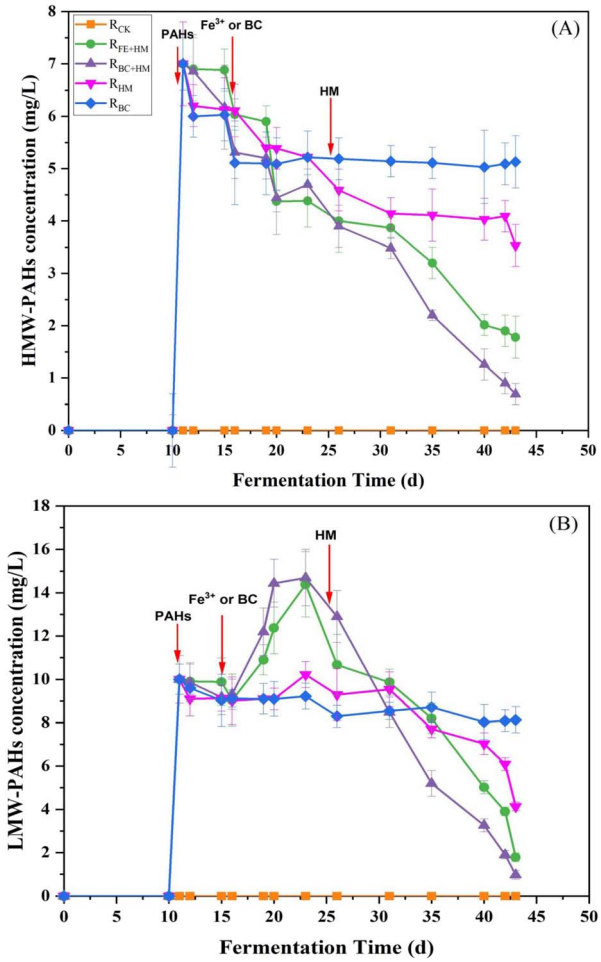

Fig. 4 Fate of HMW-PAHs (A) and LMW-PAHs (B) during the PAHs anaerobic digestion process.

the cracking of LMW-PAHs into CO_2 and methane. The toxic effect of PAHs on methanogens inhibits the final mineralization of PAHs, thereby limiting the further degradation of PAH. While HM bioaugmentation can compensate for the final mineralization step, thereby facilitating the transformation of HMW-PAHs into LMW-PAHs and consequently enhancing the overall removal rate of PAHs.[23,24] Additionally, electron transfer occurs among microbial species within anaerobic biota, laying the foundation for cooperative behaviors and community functions. Interspecies electron transfer is considered a vital process in anaerobic conditions. Therefore, improving interspecies electron transfer could be a promising approach to accelerating microbial metabolism in bioenergy applications that require interspecies electron exchange. Numerous studies have highlighted the efficacy of using conductive materials to accelerate interspecies electron transfer in biological processes.[25,26] The results obtained in this study indicated that biochar could serve as specific electron transfer mediators to improve and facilitate the electron transfer process.

In the analysis of the PAH solution by GC-MS, some PAH metabolic intermediates were detected using NIST 17 spectrum library, as shown in Table 3. The results showed that the PAH

Table 3 Metabolites detected by GC-MS

Compounds	Structure	M (g mol^{-1})
2-Pyrenol		218.25
Pyrene-7-hydroxy-8-carboxylic acid		246.26
Phenaleno[1,9-*bc*]thiophene		208.28
9,10-Phenanthrenequinone		208.21
1,9-Dihydroxy fluorene		266.25
9*H*-Fluoren-9-ol		182.22
4,5-Dimethylphenanthrene		204.27
3-Acetylphenanthrene		220.26
Anthrone		194.23
9,10-Anthracenedione		208.21
9-Fluorenone		180.2
Dibenzothiophene		184.26
2-Biphenyl acid		198.22
2-Methylnaphthalene		142.2
2-Naphthoic acid		172.18
Phthalic acid		166.13
Salicylic acid		138.12
Benzoic acid		122.12
Phenol		94.11

cyclic cracking products were detected, so the metabolic pathways of PAHs included substitution reaction and ring-opening cracking reaction. Some studies have demonstrated that the main degradation pathways of PAHs are hydroxylation, methylation, and carboxylation. The aromatic rings in PAH are reduced to produce a cyclohexane ring. The subsequent ring opening process to form aliphatic compounds is followed by multiple steps that lead to CO_2 production. The research shows that the degradation of HMW-PAHs may produce LMW-PAHs,

which was consistent with that of Yukang, Zhou *et al.* (2020).[27] It mainly undergoes the process from the first to last aromatic ring. The degradation pathway of a specific PAH needs to be further explored using individual PAH.

In order to compare the anaerobic biodegradation performance of PAHs, a review of recent literature was done about the strategies in other studies used for PAHs anaerobic biodegradation. Table 4 shows that most studies have focused on individual PAH, lacking research on mixed PAHs. Moreover, there is relatively little research on methods combining biostimulation and bioaugmentation. The results in this study indicated that the novel strategy combining hydrogenotrophic methanogens bioaugmentation and biochar biostimulation showed excellent performance in anaerobic biodegradation of mixed PAHs with above 90% of removal rate.

3.4 Microbial community analysis

3.4.1 Alpha diversity analysis. To further elucidate the impact of PAHs addition on the microbial community in the R_{CK}, R_{HM}, R_{Fe+HM}, and R_{BC+HM}, alpha diversity indexes (OTUs, Shannon, Simpson, Chao1, and coverage indexes) were introduced to validate the richness and diversity of microbial communities (Table 5).

Shannon and Simpson indexes comprehensively reflect species richness and evenness. Higher values are associated with greater evenness in species distribution, contributing to increased diversity. The Chao1 index estimates the number of species in the microbial community, indicating species richness in the sample. Coverage refers to microbial coverage, reflecting the accuracy of sequencing results in representing the actual conditions of a sample. Sobs indicate the number of species observed in a sample.

From these diversity indexes, it can be concluded that adding PAHs suppressed both the richness and evenness of the bacterial community. From this perspective, PAH addition will likely intervene in the microbial communities by blocking specific metabolic pathways. When comparing bacteria and archaea within the same group, it is evident that Shannon, Chao, and Sobs of bacteria were significantly higher than those of archaea (Table 5). These results indicated that bacterial communities exhibited higher diversity than archaeal communities under PAH inhibition. Notably, R_{BC+HM} on day 43 presented the highest Shannon index of archaea, demonstrating that combining biochar and HM can increase the diversity and richness of the microbial community.

Table 5 Alpha diversity of different samples

	Specimens	OTUs	Shannon	Simpson	Chao	Coverage
Bacteria	R_{CK}	832	3.813	0.2130	462	0.9979
	R_{BC}	806	3.112	0.0801	452	0.9969
	R_{HM}	818	3.278	0.1326	454	0.9971
	R_{BC+HM}	968	3.313	0.1378	654	0.9949
	R_{FE+HM}	925	3.363	0.1302	635	0.9949
Archaea	R_{CK}	37	1.978	0.2536	23	0.9997
	R_{BC}	22	0.850	0.1871	12	0.9946
	R_{HM}	22	0.752	0.2141	15	0.9943
	R_{BC+HM}	60	1.972	0.2646	28	0.9969
	R_{FE+HM}	38	1.336	0.2531	25	0.9968

3.4.2 Bacterial community. Fig. 5 shows that the main bacterial strains present at the genera level during PAHs biomineralization included *Streptococcus*, *norank_f__Bacteroidetes_vadinHA17*, *norank_p__Firmicutes*, *norank_c__D8A-2*, *Fastidiosipila*, *Desulfovibrio*, *Rikenellaceae_RC9_gut_group*, *norank_c__Dojkabacteria*, *Thermovirga*, and *Sedimentibacter*, which were found in all samples. *Streptococcus* was the most prevalent strain in all samples and has previously been identified in PAH-contaminated soil.[34] This bacterium is known for its ability to utilize hydrocarbons.[35] Moreover, Lei *et al.* (2016) reported a DIET syntrophy between *Streptococcus* and the hydrogenotrophic methanogen *Methanospirillum* and *Methanosarcina*.[36] *Sedimentibacter* and *Desulfovibrio* were also effective PAH-degrading bacteria.[37,38] Zhang *et al.* (2020) announced a DIET relationship between *Desulfovibrio* and

Table 4 Comparation of PAHs anaerobic biodegradation in different studies

PAHs	Strategy	Removal rates (%)	References
Phenanthrene	Granular biochar & ethanol	86.2	11
Phenanthrene, anthracene, fluoranthene, pyrene and benzo(*a*)pyrene	HCO_3^-	84.98	17
NAP, PHE, and PYR	Bioelectrochemical systems	97.60, 42.90, and 22.00	27
Phenanthrene, anthracene, fluoranthene, pyrene, and benzo[*a*]pyrene	Bicarbonate and acetate	89.67	28
Pyrene, benzo[*a*]pyrene	Pure sulfate reducing pyrene and benzo[*a*]pyrene-degrading cultures	99.6, 99.8	29
Naphthalene	Microbial electrolysis cells and bioaugmentation	94.5	30
Phenanthrene	Anaerobic sludge and granular biochar	81.0	31
∑16PAHs	Nitrogen addition	36.65	32
∑16PAHs	Nitrate & PAH degrading inoculum	76	33
∑16PAHs	Methanogenic archaea bioaugmentation using and biochar biostimulation	90	This study

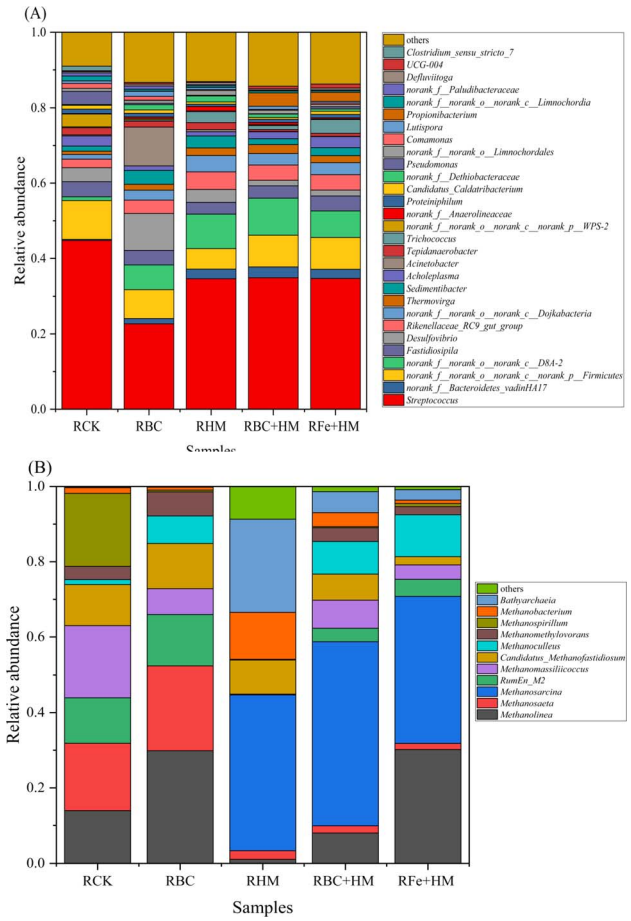

Fig. 5 Bacterial genera (A) and archaeal genera (B) in this study.

Methanosarcina in benzoate-containing wastewater.[39] Chen *et al.* (2024) reported that *Sedimentibacter* can also participate in the DIET network with hydrogenotrophic methanogen.[40] *norank_f__Bacteroidetes_vadinHA17* has been previously reported as a bacterial genus positively correlated with PAH degrading and methane production.[41] Feng *et al.* (2023) further highlighted that *norank_f__Bacteroidetes_vadinHA17* could mediate *p*-nitrophenol degradation through DIET with glucose or VFA as the electron donor.[42] Several studies have recently highlighted the significance of *norank_p__Firmicutes* in the degradation of hydrocarbons at contaminated sites.[43,44] *norank_c__D8A-2* is a typical DIET bacteria that is involved in magnetite-mediated DIET with methanogens (*Methanosaeta*, *Methanolinea*, *Methanoculleus*, and *Methanosarcina*) during VFAs degradation.[45] *Thermovirga* is also a symbiotic bacteria that works with methanogens in the digestive process, but the detailed mechanism has yet to be fully explained.[46]

After the addition of PAHs, the population of *Streptococcus* decreased. However, reactors that were treated with HM bioaugmentation along with Fe^{3+} or biochar experienced an increase in the abundance of *Streptococcus*. Similarly, the presence of *norank_c__D8A-2* increased from 1.2% in R_{CK} to 11.3% in R_{BC+HM} after the introduction of HM. It became a significant component of the microbial community in this experiment, which helped facilitate efficient VFA oxidation through DIET.

3.4.3 Archaeal community. Fig. 5 illustrates the composition of the archaeal community in different treatments, showing higher relative abundances of *Methanolinea*, *Methanosaeta*, and *Methanosarcina*. *Methanosaeta* and *Methanosarcina* are the only two known microorganisms capable of acetate methanogenesis. Methanosaeta can only use acetate as the substrate for methane production, making it an obligate acetoclastic methanogen. On the other hand, *Methanosarcina* has a versatile metabolism, which can utilize acetate and H_2/CO_2, methanol, and methylamines for methane production.[47]

A shift in dominant genera was observed after adding bioaugmentation dosage. *Methanosarcina* replaced *Methanosaeta*, becoming the predominant genus (Fig. 5). In R_{Fe+HM}, *Methanolinea* and *Methanosarcina* had relative abundances of 30.18% and 39.00%, respectively. In R_{BC+HM}, *Methanolinea* and *Methanosarcina* had relative abundances of 8.10% and 48.83%, respectively. This indicated that during the recovery process, *Methanosarcina* replaced *Methanosaeta* for methane production, restoring gas and methane production processes, especially in R_{BC+HM}. Biochar promotes syntrophic anaerobic oxidation of VFA and enriches the hydrogenotrophic archaea involved in DIET. These archaea receive electrons through VFA oxidation and reduce CO_2 to methane, facilitating methane production.[36,39,45]

3.4.4 Metabolic pathway analysis during biomineralization of PAHs. The PAH biomineralization process involves acetoclastic and hydrogenotrophic methanogenesis, converting organic PAH into inorganic methane or CO_2.[48] This study obtained enzymes participating in acetoclastic and hydrogenotrophic methanogenesis (Table 6). The functional enzymes related to above methanogenic pathways were further investigated based on KEGG database.

Through acetate methanogenesis, the resulting acetic acid is ultimately converted to methane through a series of steps (Fig. 6). Enzymes involved in acetoclastic methanogenesis were found to be lower in HM-fed reactors than in R_{CK} or R_{BC}, which was due to the origin of HM dosage as it mainly contained hydrogenotrophic methanogens.

For hydrogenotrophic methanogenesis, the process known as the Wood–Ljungdahl (WL) pathway should be emphasized due to its essential role in energy generation and carbon fixation in methanogens. Initially, hydrogenotrophic methanogens gradually reduce CO_2 to methyl-H_4MPT *via* the methyl branch of the WL pathway. The methyl group of the formed methyl-H4MPT is then transferred to coenzyme M *via* N5-methyltetrahydroleaflavin (EC 2.1.1.86) and ultimately reduced to methane and an isodisulfide (CoM-S-S-CoB) by the methyl-CoM reductase complex (EC 2.8.4.1) (Fig. 6 and Table 6).

In this study, hydrogenotrophic methanogenesis-related enzymes flourished in HM-fed reactors, particularly in R_{BC+HM}. Similarly, previous studies have emphasized the stimulating effect of PAH on hydrogenotrophic methanogenesis.[49] Based on the microbial profile (Fig. 5), the hydrogenotrophic methanogen could work syntrophically with VFA-degrading bacteria through DIET for PAH inhibition remediation and methane recovery. Notably, R_{BC+HM} enjoyed the most profound

Table 6 Predicted activities of key enzymes in this study[a]

EC number	R_{CK}	R_{HM}	R_{FE+HM}	R_{BC}	R_{BC+HM}
Acetoclastic methanogenesis					
2.7.2.1	UD	UD	UD	0.0326 ± 0.0021	0.0468 ± 0.0015
2.3.1.8	UD	UD	UD	0.0236 ± 0.0008	0.0377 ± 0.0016
6.2.1.1	0.5230 ± 0.0036	0.5160 ± 0.0061	0.5029 ± 0.0011	0.4411 ± 0.0031	0.3544 ± 0.0022
Hydrogenotrophic methanogenesis					
1.12.98.1	0.4046 ± 0.0037	0.5497 ± 0.0041	0.4248 ± 0.0037	0.3194 ± 0.0049	0.7090 ± 0.0062
1.12.98.2	UD	0.0002 ± 0.0000	UD	UD	0.0007 ± 0.0001
1.2.7.4	0.1509 ± 0.0011	0.2430 ± 0.0026	0.2275 ± 0.0036	0.1761 ± 0.0022	0.2652 ± 0.0031
1.5.98.1	0.1057 ± 0.0014	0.1110 ± 0.0018	0.1228 ± 0.0025	0.0954 ± 0.0010	0.1450 ± 0.0021
1.5.98.2	0.1308 ± 0.0029	0.1574 ± 0.0031	0.1469 ± 0.0033	0.1127 ± 0.0016	0.1584 ± 0.0010
2.1.1.86	0.8934 ± 0.0035	1.0061 ± 0.0027	1.0983 ± 0.0015	0.8282 ± 0.0025	1.2282 ± 0.0031
2.3.1.101	0.1076 ± 0.0032	0.1335 ± 0.0024	0.1253 ± 0.0033	0.0965 ± 0.0030	0.1537 ± 0.0029
2.8.4.1	0.5456 ± 0.0014	0.5852 ± 0.0019	0.5172 ± 0.0024	0.5113 ± 0.0029	0.6286 ± 0.0024
3.5.4.27	0.1751 ± 0.0037	0.1436 ± 0.0028	0.1592 ± 0.0017	0.1196 ± 0.0021	0.1655 ± 0.0025
Wood-Ljungdahl pathway					
1.5.1.20	0.1551 ± 0.0025	0.1963 ± 0.0017	0.1218 ± 0.0018	0.1478 ± 0.0013	0.2194 ± 0.0027
1.5.1.5	0.0041 ± 0.0011	0.0353 ± 0.0021	0.0137 ± 0.0027	0.0027 ± 0.0009	0.0520 ± 0.0022
1.17.1.10	0.1551 ± 0.0018	0.1963 ± 0.0036	0.1218 ± 0.0028	0.1803 ± 0.0051	0.2662 ± 0.0026
2.3.1.169	0.0755 ± 0.0018	0.0968 ± 0.0027	0.0541 ± 0.0029	0.0888 ± 0.0031	0.1305 ± 0.0027
3.5.4.9	0.1233 ± 0.0031	0.1138 ± 0.0027	0.1010 ± 0.0027	0.1338 ± 0.0014	0.2039 ± 0.0023
6.3.4.3	ND	ND	ND	ND	ND

[a] ND: under detection limit.

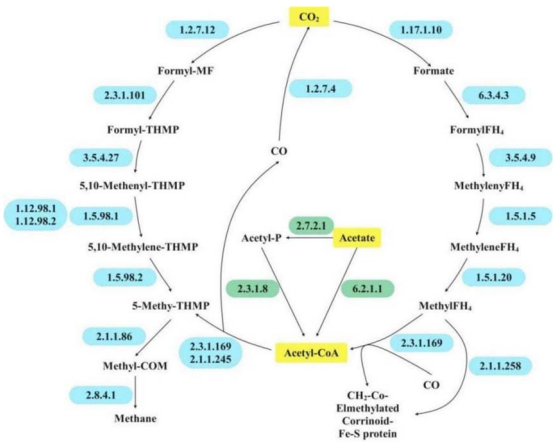

Fig. 6 Putative metabolic pathway in this study.

hydrogenotrophic methanogenesis-related enzyme activities among the tested samples (Table 6). Consequently, the higher activity of EC 2.8.4.1 was obtained in R_{BC+HM}, which compared well with its highest restored methane yield (Fig. 1).

4. Conclusions

Adding terminal electron acceptors (Fe^{3+} or biochar) coupled with hydrogenotrophic methanogens rapidly alleviated PAHs inhibition and restored biogas production capability. R_{BC+HM} showed the highest PAHs removal efficiency, with 90.1% for HMW-PAHs and 90.3% for LMW-PAHs, respectively. Consequently, R_{BC+HM} exhibited the highest restored cumulative methane production. The coupling of biochar with hydrogenotrophic methanogens restored the archaeal community's richness, leading to more efficient degradation of PAHs. Biochar and hydrogenotrophic methanogen promoted syntrophic anaerobic oxidation of VFA by enriching DIET-related microbiomes, further enhancing methane production.

Data availability

Data for this article, including figures and tables are available within the manuscript and its additional files.

Author contributions

Rui Tang: conceptualization, methodology, writing – original draft, investigation. Min Zhang: conceptualization, formal analysis. Xin Li: conceptualization, supervision, writing – original draft, writing – review & editing, funding acquisition.

Conflicts of interest

The authors declare there is no conflict.

Acknowledgements

The team would like to thank the support from the Key Laboratory of Clean Production and Utilization of Renewable Energy, Ministry of Agriculture and Rural Affairs, China Agricultural University; National Center for International Research of Bio-Energy Science and Technology, Ministry of Science and Technology, China Agricultural University; and Beijing Municipal Key Discipline of Biomass Engineering.

References

1 G. Pagnozzi, S. Carroll, D. D. Reible and K. Millerick, *Environ. Pollut.*, 2021, **268**, 115641.
2 R. Forján, I. Lores, C. Sierra, D. Baragaño, J. L. R. Gallego and A. I. Peláez, *Appl. Sci.*, 2020, **10**, 2837.
3 J. Luo, L. Wu, Y. Chen, L. Feng and J. Cao, *J. Hazard. Mater.*, 2019, **365**, 322–330.
4 M. Sharma, A. Nandy, N. Taylor, S. V. Venkatesan, V. Ozhukil Kollath, K. Karan, V. Thangadurai, N. Tsesmetzis and L. M. Gieg, *J. Hazard. Mater.*, 2020, **389**, 121845.
5 J. Liu, A. N. Zhang, Y. J. Liu, Z. Liu, Y. Liu and X. J. Wu, *Ecotoxicol. Environ. Saf.*, 2021, **225**, 112789.
6 Q. Leng, J. Mu and G. Yang, *Environ. Pollut.*, 2021, **284**, 117210.
7 A. M. Himmelberg, T. Brüls, Z. Farmani, P. Weyrauch, G. Barthel, W. Schrader and R. U. Meckenstock, *Environ. Microbiol.*, 2018, **20**, 3589–3600.
8 Z. Zhang, H. Guo, J. Sun and H. Wang, *J. Hazard. Mater.*, 2020, **383**, 121191.
9 H. Ribeiro, T. de Sousa, J. P. Santos, A. G. G. Sousa, C. Teixeira, M. R. Monteiro, P. Salgado, A. P. Mucha, C. M. R. Almeida, L. Torgo and C. Magalhães, *Chemosphere*, 2018, **199**, 54–67.
10 D. R. Lovley, *Annu. Rev. Microbiol.*, 2017, **71**, 643–664.
11 Y. Shi, H. Xue, Y. Yao, C. Jing, R. Liu, Q. Niu and H. Lu, *Chem. Eng. J.*, 2023, **477**, 147229.
12 N. Haleyur, E. Shahsavari, S. S. Jain, E. Koshlaf, V. B. Ravindran, P. D. Morrison, A. M. Osborn and A. S. Ball, *J. Environ. Manage.*, 2019, **238**, 49–58.
13 J. Mu, Q. Leng, G. Yang and B. Zhu, *Mar. Pollut. Bull.*, 2021, **167**, 112294.
14 S. Kumari, R. K. Regar and N. Manickam, *Bioresour. Technol.*, 2018, **254**, 174–179.
15 F. Bianco, M. Race, S. Papirio and G. Esposito, *Sci. Total Environ.*, 2020, **709**, 136141.
16 S. Wang, X. Li, R. Dong, W. Xiong, Y. Li and Y. Zhu, *Chemosphere*, 2023, **344**, 140370.
17 J. Mu, Y. Chen, Z. Song, M. Liu, B. Zhu, H. Tao, M. Bao and Q. Chen, *J. Hazard. Mater.*, 2022, **438**, 129569.
18 Y. Chen, Z. Qin, P. Zhang, X. Li and L. Feng, *Bioresour. Technol.*, 2022, **360**, 127567.
19 Y. Yao, J. Li, H. Xue, Y. Liu, J. Qiao, J. Tang, R. Liu and Q. Niu, *Sustainability*, 2022, **14**(24), 16377.
20 M. Yan, Z. Hu, Z. Duan, Y. Sun, T. Dong, X. Sun, F. Zhen and Y. Li, *Water Res.*, 2023, **246**, 120711.
21 J. Zhao, Y. Li and G. J. W. Euverink, *Chem. Eng. J.*, 2022, **428**, 131015.
22 X. Li, Z. Yu, Q. Chen, C. Wang, L. Ma and G. Shen, *Chem. Eng. J.*, 2022, **430**, 132844.
23 S. B. Larsen, D. Karakashev, I. Angelidaki and J. E. Schmidt, *J. Hazard. Mater.*, 2009, **164**, 1568–1572.
24 A. Ferraro, G. Massini, V. M. Miritana, A. Panico, L. Pontoni, M. Race, S. Rosa, A. Signorini, M. Fabbricino and F. Pirozzi, *Chemosphere*, 2021, **275**, 130091.
25 L. Yu, Y. Yuan, J. Tang, Y. Wang and S. Zhou, *Sci. Rep.*, 2015, **5**, 16221.
26 S. Chen, A. E. Rotaru, P. M. Shrestha, N. S. Malvankar, F. Liu, W. Fan, K. P. Nevin and D. R. Lovley, *Sci. Rep.*, 2014, **4**(1), 5019.
27 Y. Zhou, Q. Zou, M. Fan, Y. Xu and Y. Chen, *J. Hazard. Mater.*, 2020, **381**, 120945.
28 Q. Chen, Z. Li, Y. Chen, M. Liu, Q. Yang, B. Zhu and Z. Chen, *Mar. Pollut. Bull.*, 2024, **199**, 115925.
29 Z. Zhang, J. Sun, X. Gong, C. Wang and H. Wang, *J. Hazard. Mater.*, 2023, **459**, 132053.
30 Z. Min, T. Rui and L. Yu, *Water Sci. Technol.*, 2024, **89**(10), 2716–2731.
31 H. Xue, Y. Shi, J. Qiao, X. Li and R. Liu, *Sustainability*, 2023, **16**(1), 366.
32 S. Yuan, X. Han, X. Yin, P. Su, Y. Zhang, Y. Liu and D. Zhang, *Sci. Total Environ.*, 2023, **864**, 161034.
33 N. Zhou, Z. Yang, J. Zhang, Z. Zhang and H. Wang, *Bioresour. Technol.*, 2024, **393**, 130090.
34 A. Janbandhu and M. H. Fulekar, *J. Hazard. Mater.*, 2011, **187**, 333–340.
35 C. E. Achife, U. J. J. Ijah, S. B. Oyeleke, J. D. Bala, O. A. Oyewole, N. R. Maddela and R. Prasad, *Appl. Biochem. Biotechnol.*, 2024, **196**, 2819–2838.
36 Y. Lei, D. Sun, Y. Dang, H. Chen, Z. Zhao, Y. Zhang and D. E. Holmes, *Bioresour. Technol.*, 2016, **222**, 270–276.
37 Y. Qian, M. Xu, T. Deng, W. Hu, Z. He, X. Yang, B. Wang, D. Song, L. Chen, Y. Huang and G. Sun, *J. Hazard. Mater.*, 2021, **407**, 124385.
38 H. Cai, L. Sun, Y. Wang, T. Song, M. Bao and X. Yang, *Chem. Eng. J.*, 2019, **369**, 1078–1092.
39 F. Zhang, D.-K. Qian, X.-B. Wang, K. Dai, T. Wang, W. Zhang and R. J. Zeng, *Sci. Total Environ.*, 2020, **723**, 138080.
40 S. Chen, F. Yao, Z. Pi, L. He, K. Luo, X. Li and Q. Yang, *Environ. Manage.*, 2024, **351**, 119911.
41 Y.-Q. Wang, M.-X. Wang, Y.-Y. Chen, C.-M. Li and Z.-F. Zhou, *J. Hazard. Mater.*, 2021, **417**, 126086.
42 Y. Feng, J. Lu, Z. Shen, J. Li, H. Zhang, X. Cao, Z. Ye, G. Ji, Q. Liu, Y. Hu and B. Zhang, *J. Hazard. Mater.*, 2023, **451**, 131055.
43 C. Berdugo-Clavijo, X. Dong, J. Soh, C. W. Sensen and L. M. Gieg, *FEMS Microbiol. Ecol.*, 2012, **81**, 124–133.
44 U. Kunapuli, M. K. Jahn, T. Lueders, R. Geyer, H. J. Heipieper and R. U. Meckenstock, *Int. J. Syst. Evol. Microbiol.*, 2010, **60**, 686–695.
45 J. Lee, T. Koo, A. Yulisa and S. Hwang, *J. Environ. Manage.*, 2019, **241**, 418–426.
46 Z. Wang, C. Zhang, J. Watson, B. K. Sharma, B. Si and Y. Zhang, *Chem. Eng. J.*, 2022, **435**, 135078.
47 T. D. Mand and W. W. Metcalf, *Microbiol. Mol. Biol. Rev.*, 2019, **83**(4), e000200.
48 S. V. Mohan, T. Kisa, T. Ohkuma, R. A. Kanaly and Y. Shimizu, *Rev. Environ. Sci. Bio/Technol.*, 2006, **5**, 347–374.
49 H. Wang, L. Lu, X. Chen, Y. Bian and Z. J. Ren, *Water Res.*, 2019, **164**, 114942.